Chemical Research in Toxicology

Article

Cite This: Chem. Res. Toxicol. XXXX, XXX, XXX−XXX

pubs.acs.org/crt

Metabolic Activation of Elemicin Leads to the Inhibition of Stearoyl-CoA Desaturase 1

Xiao-Nan Yang,[†,⊥,▽] Yi-Kun Wang,[†,‡,▽] Xu Zhu,[†,‡] Xue-Rong Xiao,[†] Man-Yun Dai,[†,‡] Ting Zhang,[†,‡] Yan Qu,[†] Xiu-Wei Yang,[§] Hong-Bo Qin,[†] Frank J. Gonzalez,[∥] and Fei Li*[,†]

[†]States Key Laboratory of Phytochemistry and Plant Resources in West China, Kunming Institute of Botany, Chinese Academy of Sciences, Kunming 650201, China

[‡]University of Chinese Academy of Sciences, Beijing 100049, China

[§]School of Pharmaceutical Sciences, Peking University Health Science Center, Peking University, Beijing 100191, China

[∥]Laboratory of Metabolism, Center for Cancer Research, National Cancer Institute, National Institutes of Health, Bethesda, Maryland 20892, United States

[⊥]Guangxi Key Laboratory of Medicinal Resources Protection and Genetic Improvement, Guangxi Botanical Garden of Medicinal Plant, Nanning 530023, China

Supporting Information

ABSTRACT: Elemicin is a constituent of natural aromatic phenylpropanoids present in many herbs and spices. However, its potential to cause toxicity remains unclear. To examine the potential toxicity and associated mechanism, elemicin was administered to mice for 3 weeks and serum metabolites were examined. Enlarged livers were observed in elemicin-treated mice, which were accompanied by lower ratios of unsaturated- and saturated-lysophosphatidylcholines in plasma, and inhibition of stearoyl-CoA desaturase 1 (*Scd1*) mRNA expression in liver. Administration of the unsaturated fatty acid oleic acid reduced the toxicity of 1′-hydroxylelemicin, the primary oxidative metabolite of elemicin, while treatment with the SCD1 inhibitor A939572 potentiated its toxicity. Furthermore, the in vitro use of recombinant human CYPs and chemical inhibition of CYPs in human liver microsomes revealed that CYP1A1 and CYP1A2 were the primary CYPs responsible for elemicin bioactivation. Notably, the CYP1A2 inhibitor α-naphthoflavone could attenuate the susceptibility of mice to elemicin-induced hepatomegaly. This study revealed that metabolic activation of elemicin leads to SCD1 inhibition in liver, suggesting that upregulation of SCD1 may serve as potential intervention strategy for elemicin-induced toxicity.

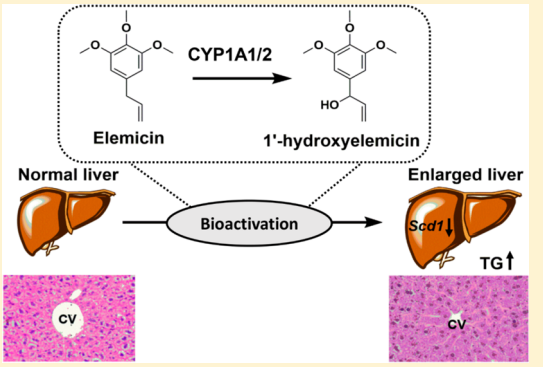

INTRODUCTION

Alkenylbenzenes are naturally occurring compounds composed of a benzene ring with a carbon chain (C6−C3 moiety). Elemicin (3,4,5-trimethoxyallylbenzene) is a typical alkenylbenzene that is widely distributed in various medicinal plants, including nutmeg (*Myristica fragrans* Houtt.), parsley [*Petroselinum crispum* (Mill.) A. W. Hill], *Asarum heterotropoides*, sassafras [*Sassafras albidum* (Nutt.)], and *Canarium commune*.[1,2] Elemicin is one of the main components in aromatic food supplemented in baked goods, meats, nonalcoholic beverages, or ice creams.[3] Recently, elemicin has attracted much attention owing to its extensive pharmacological potential, including antimicrobial,[4] antioxidant,[5] and antiviral[6] activities. However, as an alkenylbenzenes, elemicin is similar to estragole, safrole, methyleugenol and myristicin, that cause genotoxicity[7] and hepatocarcinogenic effects in rodent models.[8−10] It was previously revealed that 1′-hydroxylation of alkenylbenzenes could generate electrophilic derivatives such as 1′-hydroxyestragole and 1′-hydroxysafrole.[11,12] These metabolites can react with DNA and form genotoxic carcinogens. However, the potential toxicity of elemicin remains unclear.[9,13,14]

Diversified alkenylbenzenes included estragole, myristicin, and elemicin were reported to possess genotoxicity and carcinogenicity.[15] The 1′-hydroxylated metabolites of these alkenylbenzenes mostly showed potent reactivity and thus may play an initial role in the genotoxicity of the parent compounds.[9,12,14,16] Recently, an in vitro model revealed that low levels of the procarcinogenic metabolites 1′-hydroxyelemicin and 1′-sulfoxyelemicin could be formed from elemicin.[17] Nevertheless, large doses or long-term consumption of elemicin or foods rich in elemicin may cause genotoxicity.[13] However, the risk assessment data on elemicin or 1′-hydroxyelemicin on liver are limited.

Received: March 15, 2019
Published: August 30, 2019

DOI: 10.1021/acs.chemrestox.9b00112
Chem. Res. Toxicol. XXXX, XXX, XXX−XXX

In the present study, a mass spectrometry-based metabolomic approach was adopted to study elemicin-induced toxicity and its mechanism. Metabolic changes were investigated in mice after a three-week daily exposure to 500 mg/kg elemcin. A significant inhibitory effect of elemcin exposure on stearoyl-CoA desaturase 1 (SCD1) was identified in mouse liver, leading to hepatomegaly. 1′-Hydroxyelemicin administration triggered a disruption of hepatic lipid homeostasis, which could be potentiated by the SCD1 inhibitor A939572 and ameliorated by supplementation of mouse diets with oleic acid. The CYP1A2 inhibitor α-naphthoflavone attenuated the hepatomegaly of elemicin in mice. Further experiments identified CYP1A1 and CYP1A2 as the major CYP responsible for the metabolic activation of elemicin. These data suggested that metabolic activation of elemicin contributes to its toxicity.

MATERIALS AND METHODS

Chemicals and Reagents. Elemicin was purchased from Maya Reagent (Jiaxing, China), and 1′-hydroxyelemicin was synthesized by Hong-Bo Qin's laboratory in the Kunming Institute of Botany (Supporting Information). NADPH, chlorpropamide, and formic acid were purchased from Sigma-Aldrich (St. Louis, MO, U.S.A.). Human liver microsomes (HLMs) were obtained from Bioreclamationivt Inc. (Hicksville, NY, U.S.A.) and recombinant human CYPs provided by Xenotech, LLC (Kansas City, KS, U.S.A.). α-Naphthoflavone, trimethoprim, and quinidine were obtained from the Shanghai Macklin Biochemical Co., Ltd. (Shanghai, China). Methoxsalen, ticlopidine, and ketonazole were purchaed from Dalian Meilun Biotechnology Co., Ltd. (Dalian, China). Sulfaphenazol was from MedChemExpress LLC (Shanghai, China). The triglyceride (TG) kit was purchased from Nanjing Jiancheng Bioengineering Institute (Nanjing, China). TRIzol reagent for total RNA extraction was obtained from Invitrogen (Carlsbad, CA, U.S.A.). Monoclonal rabbit anti-SCD1 (2794S) and monoclonal rabbit anti-GAPDH (2118S) were obtained from Cell Signaling Technology (Danvers, MA, U.S.A.). HRP-conjugated Affinipure Goat Anti-Rabbit (SA0001-2) was purchased from Proteintech Group (Manchester, U.K.). SCD1 inhibitor A939572 was obtained from Bide Pharmatech Ltd. (Shanghai, China). AIN93 M purified diet and high-oleic acid diet were sourced from Biotech HD Co., Ltd. (Beijing, China). All other reagents and solvents were of the highest grade commercially available.

Animal Experiment and Sample Collections. Male 20−22 g wild-type C57BL/6J mice were purchased from the Kunming Institute of Zoology, Chinese Academy of Sciences (Yunnan, China). The mice were housed in cages at 23 ± 1 °C, with humidity 50−60% and a 12 h/12 h of light/dark cycle for at least 1 week. All animal studies were performed under study procedures that were preapproved by the Ethics Review Committee for Animal Experimentation of the Kunming Institute of Botany, Chinese Academy of Sciences.

Experiment 1. The toxicity of elemicin was evaluated in mice. Ten mice were randomly divided into two groups (n = 5). One group was orally administered by gavage 0.5% sodium carboxymethyl cellulose (CMC-Na) solution as the vehicle control (defined as EC group), and the other group was treated with 500 mg/kg of elemicin suspended in 0.5% CMC-Na, and defined as the E group. The dosage of elemicin was optimized in a previous study.[18] Treatment was conducted every 24 h for 3 weeks continuously. The whole blood was collected with an anticoagulative tube by retro-orbital bleeding at 24 h after the last treatment. Plasma samples were obtained by centrifugation of whole blood at 2000g for 5 min at 4 °C. Mice were then killed by CO_2 asphyxiation, and liver tissues were excised and weighed. The hepatic index was calculated as Hepatic index = (liver weight/body weight) × 100. A portion of liver was excised and preserved in 10% buffered formalin for histological analysis, and the other part of liver tissue was flash frozen in liquid nitrogen for qPCR and Western blot analysis.

Experiment 2. The toxicity of 1′-hydroxyelemicin was also assessed using C57BL/6J mice. Total 12 mice were randomly divided into two groups (n = 6). One group of mice were treated with 0.5% CMC-Na as vehicle control (defined as E′C group), and the other group was administered 100 mg/kg of 1′-hydroxyelemicin (defined as E′ group) every 24 h for 3 days. After 24 h of the last treatment, plasma and liver samples were collected and processed according to the experiment 1.

Experiment 3. A modified AIN93 M diet containing 20 g/kg oleic acid (OA) and 20 g/kg soybean oil was used as the high-oleic acid diet. An AIN93 M purified diet containing 40 g/kg soybean oil was used as the control diet. All mice were acclimated to the AIN93 M control diet at the beginning of the experiment. After 1 week, one group of mice (defined as the OA+ E′ group, n = 4) received the high-oleic acid diet for 3 days while the other two groups of mice (defined as E′C or E′ group, n = 4, respectively) were fed the control diet continuously. Then mice of OA + E′ and E′ group were orally treated with 100 mg/kg of 1′-hydroxyelemicin for another 3 days, and the mice of control group received 0.5% of CMC-Na as vehicle solvent. After 24 h of the last treatment, plasma and liver samples were collected and processed according to the experiment 1.

Experiment 4. C57BL/6J mice were randomly divided into 3 groups (E′C, E′ and A + E′ group, n = 4) for SCD1 suppression experiment. A synthesized SCD1 inhibitor A939572 was dissolved in a mixed solvent (DMSO/tween 80/saline = 1:2:97), and intraperitoneally injected twice a day at a dose of 10 mg/kg/day (defined as A + E′ group). The mice in A + E′ and E′ groups received 100 mg/kg of 1′-hydroxyelemicin orally every 24 h for 3 times after the first dose of A939572 or vehicle solution. Then, 24 h after the last treatment, plasma and liver samples were collected and processed according to the experiment 1.

Experiment 5. the role of metabolic activation in the toxicity of elemicin was evaluated. Fifteen mice were randomly divided into three groups (EC, E and N + E group, n = 5). The CYP1A1/2 inhibitor alpha-naphthoflavone was dissolved in corn oil, and intraperitoneally injected once a day at a dose of 80 mg/kg/day (defined as A + E′ group). The mice in N + E and E groups received 500 mg/kg of elemicin orally every 24 h for 7 days after the first dose of alpha-naphthoflavone or vehicle solution. Plasma and liver samples were collected at 24 h after the last treatment, and processed according to the experiment 1.

Experiment 6. Comparison of elemicin and 1′-hydroxyelemicin toxicity at the same dose of 100 mg/kg for 3 days were tested in mice. Fifteen mice were randomly divided into three groups (EC, E and E′ group, n = 5). EC group was administered 0.5% CMC-Na. E and E′ groups were treated with 100 mg/kg of elemicin and 1′-hydroxyelemicin, respectively. Plasma and liver samples were collected at 24 h after the last treatment.

Histological and Biochemical Analysis. Liver H&E staining were carried out according to a previous report.[19] The TG contents in mouse plasma and liver were measured colorimetrically using a commenrcial kit (Jiancheng Bioengineering Institute, Nanjing, China) according to the venders manual.

UPLC-ESI-QTOFMS-Based Metabolomics Analysis. Samples for UPLC-ESI-QTOFMS metabolomics analysis were prepared according to a previous report.[19] The endogenous metabolites were extracted by adding 10 μL of plasma into 190 μL of 67% acetonitrile containing the internal standard 5 μM chlorpropamide, and vortexed for 1 min and the samples centrifuged at 18000g for 20 min at 4 °C. The injection volume of supernatant was 5 μL for UPLC-ESI-QTOFMS analysis. The working condition of the UPLC-ESI-QTOFMS was the same as employed in a previous report.[20] Endogenous metabolites were identified by searching the online databases (METLIN and HMDB) and according to a previous report.[19] The abundance of GSH and GSSG in plasma was measured by an LC-MS equipped with hydrophilic Hilic column. The qualitative identification of GSH and GSSG was achieved by comparing the chromatographic behavior and MS/MS with the reference substances.

Detection of Reactive Metabolite-GSH Adduct in Vivo and in Vitro. 1′-Hydroxyelemicin plus GSH adduct ($C_{22}H_{31}N_3O_{10}S$,

DOI: 10.1021/acs.chemrestox.9b00112
Chem. Res. Toxicol. XXXX, XXX, XXX−XXX

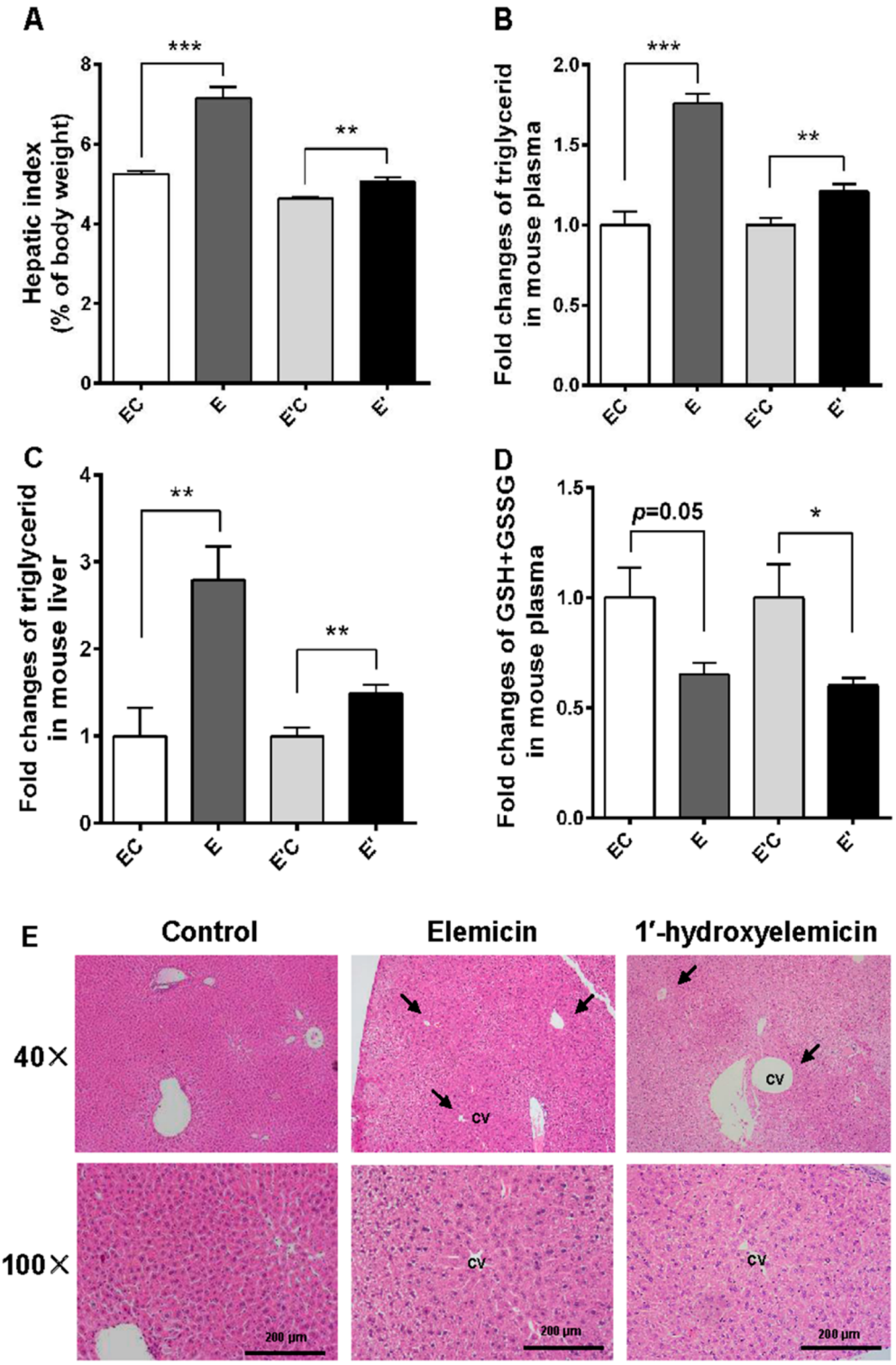

Figure 1. 1′-Hydroxyelemicin showed similar toxicity-induced by elemicin in mice. (A) Hepatic index after elemicin (E) and 1′-hydroxyelemicin (E′) treatment. (B) Levels of plasma TG. (C) Levels of hepatic TG. (D) Levels of total reduced glutathione (GSH) and oxidized glutathione (GSSG). (E) Histological results of mouse liver. *, $p < 0.05$, **, $p < 0.01$, ***, $p < 0.001$.

observed $[M + H]^+ = 530.1684$) was detected using UPLC-MS/MS. 1′-Hydroxyelemicin eluted at 5.28 min and was identified by a characteristic MS/MS ion at m/z 225 (protonated1′-hydroxyelemicin moiety corresponding to losses of GSH).

Two separate trapping experiments were in vitro conducted to detect the 1′-hydroxyelemicin-GSH adduct. The incubation mixtures were in a final volume of 200 μL PBS, containing 0.5 mg/mL of MLMs, 50 μM of elemicin, and 1 mM of NADPH. Details for the incubations were operated according to a published procedure.[23] To further confirm the chemically reactive activity of 1′-hydroxyelemicin, incubation of synthesized 1′-hydroxyelemicin with 1 mM GSH in PBS at room temperature for 40 min, without any addition of MLMs. The resulting incubates were subjected to UPLC-MS/MS to measure the formation of the elemicin-derived-GSH conjugate.

Gene Expression Analysis. Messenger RNA quantification was performed by quantitative RT-PCR. The experimental detaiels are in

DOI: 10.1021/acs.chemrestox.9b00112
Chem. Res. Toxicol. XXXX, XXX, XXX−XXX

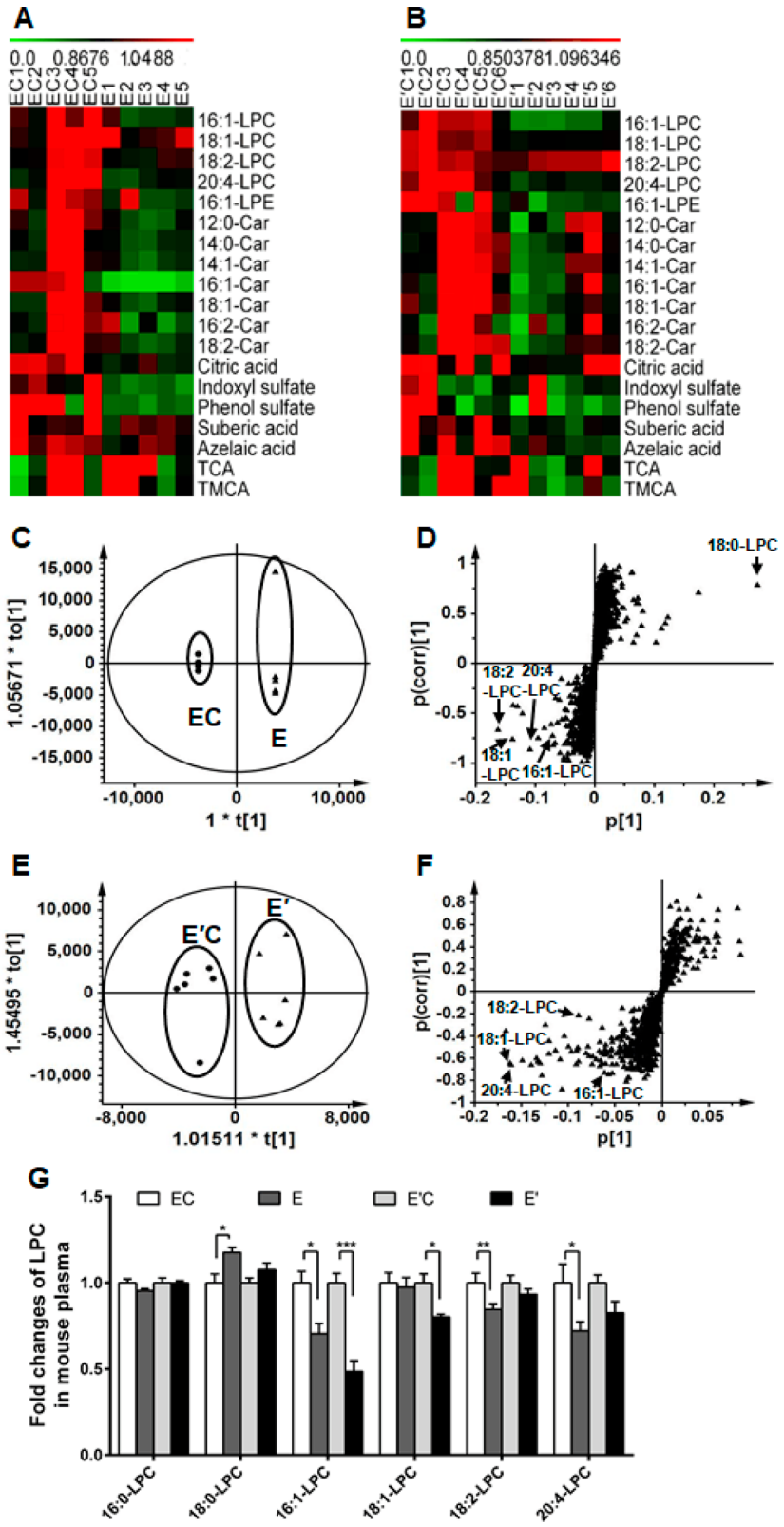

Figure 2. Metabolomics analysis of plasma from elemicin- and 1′-hydroxyelemicin-treated mice. (A) Heat map analysis of the changed endogenous metabolites after elemicin treatment. (B) Heat map analysis of the changed endogenous metabolites after 1′-hydroxyelemicin treatment. (C) OPLS-DA model of plasma samples from vehicle group (EC) and elemicin-treated group (E). (D) Loading scatter plot of OPLS-DA model of EC and E. (E) OPLS-DA model of plasma samples from vehicle group (E′C) and 1′-hydroxyelemicin-treated group (E′). (F) Loading scatter plot of OPLS-DA model of E′C and E′. (G) Alteration of LPCs in mouse plasma after elemicin and 1′-hydroxyelemicin treatment. Metabolites contributing to the separation of two groups were labeled. *, $p < 0.05$, **, $p < 0.01$.

DOI: 10.1021/acs.chemrestox.9b00112
Chem. Res. Toxicol. XXXX, XXX, XXX−XXX

accordance with a previous report.[19] The qPCR primer sequences are listed in Table S1.

Western Blot Immunoassay. Fresh liver tissue was isolated and homogenized in RIPA buffer supplemented with PMSF for whole protein samples extraction according to the manufacturer's instructions. After completing cell lysis, the whole homogenate was centrifuged at 12 000 rpm for 20 min. The concentration of total protein was determined using the BCA Protein Assay kit. Then, 10 μg of each protein sample was separated by 10% SDS-PAGE gel and transferred to PVDF membranes using the Semi-Dry Trans-Blot Turbo (Bio-Rad Laboratories, Hercules, CA, U.S.A.). The membranes were washed with 0.5% Tween 20 in 1× Tris-buffered saline (TBS/T) and blocked for 2.5 h at room temperature with blocking buffer. Blocked membranes were incubated overnight at 4 °C with primary antibodies, washed fore times for 10 min each in TBS/T and incubated with the secondary antibody for 2 h at room temperature, followed by detection using an ECL detection system according to the manufacturer's instructions.

Contribution of CYPs to Elemicin Metabolism. The in vitro metabolism of elemicin was conducted in a 96 wells plate. The total 200 μL incubation system contained 50 μM of elemicin, 10 nmol/L of each c-DNA-expressed CYPs (including control protein, CYP1A1, CYP1A2, CYP1B1, CYP2A6, CYP2B6, CYP2C19, CYP2C8, CYP2C9, CYP2D6, CYP2E1, CYP3A4, CYP3A5, and CYP4A11) and 1 mM of NADPH (final concentration) in phosphate buffer saline (pH 7.4). The incubation process and sample preparation of CYPs were consistent with the previous report.[20] All incubations were conducted in triplicate.

In addition, the inhibition study was performed by using pooled mouse liver microsomes (MLMs). The incubation systems contained (final concentration) 0.5 mg/mL protein, 50 μM of elemicin, 1 mM NADPH and each inhibitor in total volume of 200 μL (PBS system, pH 7.4). The chemical inhibitors in acetonitrile were added as follows: α-naphthoflavone (1 μM for CYP1A1/2), methoxsalen (20 μM for CYP2A6), ticlopidine (100 μM for CYP2B6 and 2C19), trimethoprim (100 μM for CYP2C8), sulfaphenazole (20 μM for CYP2C9), quinidine (5 μM for CYP2D6), 4-methylpyrazole (100 μM for CYP2E1), and ketoconazole (10 μM for CYP3A4). The concentrations of inhibitors were determined according to previous reports.[21,22] After preincubation of MLMs with each inhibitor for 5 min, a final concentration of 50 μM elemicin was added to the incubations. The reactions were terminated after 40 min by adding 200 μL of ice-cold acetonitrile. Samples for UPLC-ESI-QTOFMS analysis were prepared, according to the description above.

To calculate the V_{max} and K_m values of CYPs for catalyzing 1′-hydroxylation of elemicin, human recombinant CYP1A1, CYP1A2, CYP2A6, CYP2C19, and CYP3A4 were separately incubated with elemicin ranging from 0 to 300−500 μM in triplicates. Production of 1′-hydroxyelemicin was quantified by UPLC-ESI-QTOFMS using a standard curve of the pure compound. Kinetic constants for the metabolic conversions of elemicin was derived by fitting the data to the standard Michaelis−Menten equation, $v = V_{max} \times [S]/K_m + [S]$. The in vitro catalytic efficiency was calculated as $1000\ \mu L \times V_{max}/K_m$.

Prediction of the Affinities of Elemicin by Molecular Docking. Molecular Operating Environment 2014 (MOE, version 2014.11; Chemical Computing Group Inc., Montreal, QC, Canada) was used for molecular docking to elucidate the affinities between elemicin and human CYP isomers. The standard two-dimensional structure of ligand (elemicin) was drew in Chem Bio Draw 12.0 software. The crystal structure of receptors included CYP 1A1 (PDB ID: 4i8v, resolution: 2.6 Å), 1A2 (PDB ID: 2hi4, resolution: 1.95 Å), 2A6 (PDB ID: 1z11, resolution: 2.05 Å), 2C19 (PDB ID: 4gqs, resolution: 2.87 Å), and 3A4 (PDB ID: 4NY4, resolution: 2.95 Å), was obtained from the protein data bank. The residue process were consistent with the previous report.[23]

Statistical Analysis. All data were presented as mean ± SEM. Statistical analysis was performed using GraphPad Prism vision 6.01 (GraphPad Software, San Diego, CA, U.S.A.). $p < 0.05$ was determined as the significant differences.

RESULTS

Elemicin and Its Reactive Metabolite of 1′-Hydroxyelemicin Induced Hepatotoxicity. Compared with the control group, liver weights were increased after oral administration of elemicin for 3 weeks (Figure 1A), with no significant changes in serum ALT (Figure S1). TG levels in plasma and liver were significantly elevated in mice treated with elemicin (Figure 1B,C), while the total plasma GSH and GSSG were reduced (Figure 1D), suggesting that elemicin exposure for 3 weeks impaired liver function. Similarly, liver weights and plasma and liver TG in 1′-hydroxyelemicin-treated mice were higher than those in control vehicle-treated mice. The total GSH and GSSG levels were also reduced in mice by 1′-hydroxyelemicin treatment. Histopathological analysis of hepatic tissue revealed normal gross histology in the control group while the elemicin- and 1′-hydroxyelemicin-treated groups exhibited cytoplasmic pale staining, hepatocyte swelling and the cytoplasm seemed abnormal around the central vein (Figure 1E). The observed hepatomegaly was likely due to microsteatosis. These results demonstrated that the enlarged the liver size after elemicin treatment is due in part to expansion of hepatocyte volume and increase in hepatic TG. Additionally, the liver index in 100 mg/kg 1′-hydroxyelemicin treatment was higher than that found with the same dose of elemicin, suggesting a higher toxicity of 1′-hydroxyelemicin compared to elemicin (Figure S2).

1′-Hydroxyelemicin Was Conjugated with GSH. 1′-Hydroxyelemicin plus its GSH adduct were initially observed in the urine after treatment with 100 mg/kg 1′-hydroxyelemicin, suggesting a role of GSH in the elemicin-induced toxicity following metabolic-activation. *In vitro* capture reactions in MLMs, incubation with 1′-hydroxyelemicin and GSH generated an electrophilic intermediate of elemicin (Figure S3A). To determine the chemical characteristics of 1′-hydroxyelemicin, spontaneous binding reaction was found between 1′-hydroxyelemicin and GSH (Figure S3B). These results demonstrated that 1′-hydroxyelemicin was the key reactive metabolite of elemicin, and could covalent bind with GSH, which corresponded to the exhaustion of GSH and GSSH in plasma in elemicin-treated mice.

Metabolomics Revealed Inhibition of SCD1 by Elemicin and 1′-Hydroxyelemicin. Endogenous metabolites that were changed by elemicin and 1′-hydroxyelemicin were analyzed using a UPLC-ESI-QTOFMS-based metabolomics approach. Clustering analysis showed that the levels of various endogenous metabolites in plasma were significantly altered by elemicin or 1′-hydroxyelemicin, including phospholipids, acylcarnitines and some intestinal flora-derived metabolites (Figure 2A,B). Orthogonal partial least-squares-discriminate analysis (OPLS-DA) demonstrated that the plasma sample data set from control group (EC) and elemicin group (E), or control group (E′C) and 1′-hydroxyelemicin group (E′) were clearly separated (Figure 2C,E). In addition, the primary ions contributing to separation of elemicin and the vehicle-treated control group, as well as the 1′-hydroxyelemicin-treated and its control group, were identified as lysophosphatidylcholines (LPCs; Figure 4D,F). The relative abundance of these metabolites was normalized to internal standards. The saturated LPC (18:0-LPC) was significantly increased in the elemicin-treated mouse plasma, while unsaturated LPCs, including 18:1-LPC, 18:2-LPC, 16:1-LPC, and 20:4-LPC, were obviously reduced, compared with the

DOI: 10.1021/acs.chemrestox.9b00112
Chem. Res. Toxicol. XXXX, XXX, XXX−XXX

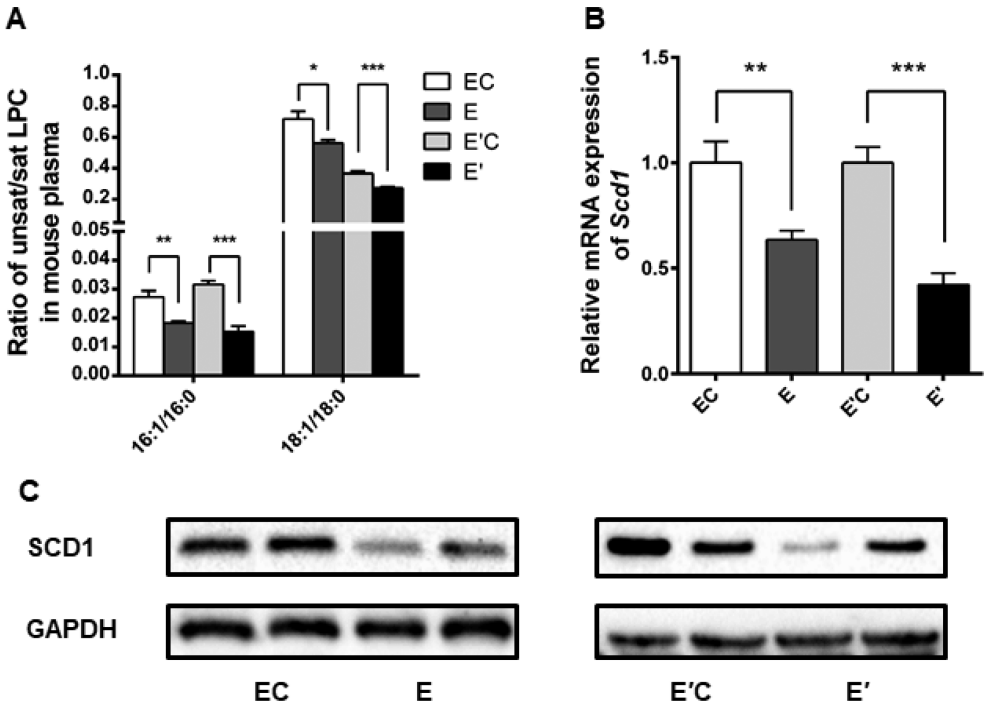

Figure 3. SCD1 was suppressed by elemicin (E) and 1′-hydroxyelemicin (E′). (A) Ratios of monounsaturated-LPCs to saturated-LPCs. (B) Relative mRNA expression of hepatic *Scd1* gene by qPCR. (C) Western blot analysis of SCD1. *, $p < 0.05$, **, $p < 0.01$, ***, $p < 0.001$.

control group. (Figure 2G). Similarly, the levels of 16:1-LPC, 18:1-LPC, and 20:4-LPC were decreased significantly in 1′-hydroxyelemicin-treated mouse plasma. The level of 18:0-LPC was slightly increased without statistical significance. The structural characterization of LPCs was performed, according to a previous report[19] and displayed in Table S2 and Figure S4.

Further, the levels of mRNAs associated with LPC biosynthesis, metabolism and hydrolysis did not show significant changes by elemicin or 1′-hydroxyelemicin treatment, including *Chpt1*, *Pcyt1a*, *Chka*, *Chkb*, *Lpcat1*, *Lpcat2*, and *Lypla1* (Figure S5). However, the ratios of oleayl-LPC (18:1-LPC) to oleoyl-LPC (18:0-LPC), palmitoleoyl-LPC (16:1-LPC) to palmitoyl-LPC (16:0-LPC) in both the elemicin- and 1′-hydroxyelemicin-treated mouse plasma were dramatically reduced, compared to the control mouse group (Figure 3A). SCD1 is an endoplasmic reticulum (ER) enzyme, responsible for the synthesis of oleic acid (C18:1) and palmitoleic acid (C16:1) from stearic acid (C18:0) and palmitic acid (C16:0) by desaturation, respectively.[24] The mRNA levels of *Scd1* were clearly decreased in the elemicin and 1′-hydroxyelemicin-treated mouse liver, compared to the control mice (Figure 3B). Moreover, Western blot analysis also revealed that SCD1 was decreased by both elemicin and 1′-hydroxyelemicin exposure (Figure 3C). These data demonstrated that elemicin and 1′-hydroxyelemicin treatment could inhibit liver SCD1, leading to a disequilibrium of LPCs.

Role of SCD1 in 1′-Hydroxyelemicin-Induced Toxicity. To determine the role of SCD1 in 1′-hydroxyelemicin-induced toxicity, the response of mice on a high-oleic acid (SCD1 substrate) diet to 1′-hydroxyelemicin treatment was investigated. TG content in plasma of high-oleic acid-fed mice recovered to normal levels, compared to 1′-hydroxyelemicin-treated mice (Figure 4A). However, the hepatic TG content and liver size in high oleic acid-fed mice were still higher than that of control mice (Figure S6A,B).

As expected, high-oleic acid feeding ameliorated the decrease of 16:1-LPC, 18:1-LPC, and 18:2-LPC levels in mouse plasma (Figure 4B). The ratios of 18:1-LPC to 18:0-LPC, 16:1-LPC to 16:0-LPC in high-oleic acid-fed mouse plasma were also increased to normal level (Figure 4C). These results demonstrated that oleic acid supplemental diet could alleviate the 1′-hydroxyelemicin-induced LPCs metabolic disorder. In contrast, the effect of the SCD1 inhibitor A939572 on 1′-hydroxyelemicin- induced liver toxicity revealed that liver size was slightly increased in the 1′-hydroxyelemicin group and A939572 plus 1′-hydroxyelemicin-treated group, but there were no significant differences between the two groups (Figure S2C). Western blot analysis demonstrated that SCD1 expression in the A + E′ group was significantly decreased (Figure 5A). TG levels in both plasma, and liver size of the A + E′ group, were markedly elevated, compared to that of the E′ group (Figure 5B and 5C). The levels of monounsaturated-LPCs in mouse plasma were further decreased in the A + E′ group (Figure 5D). The ratio of unsaturated-LPCs to saturated-LPCs was significantly reduced in the A + E′ group compared to the E′ group (Figure 5E). These results revealed that SCD1 inhibition could exacerbate the 1′-hydroxyelemicin- induced LPCs metabolic disorder.

Metabolic Activation of Elemicin by CYPs. To clarify the role of various metabolic enzymes in the formation of 1′-hydroxyelemicin, individual recombinant human CYPs were incubated with elemicin. Among the tested enzymes, CYP1A1 exhibited the strongest catalytic activity toward 1′-hydroxyelemicin generation; the proportion of 1′-hydroxyelemicin generated by CYP1A1 was 48%, while fo CYP1A2 generated 13% of 1′-hydroxyelemicin and CYP2C19 generated 9.0% of 1′-hydroxyelemicin (Figure 6B). In addition, the percentage inhibitory effects of the different CYP chemical inhibitors revealed that the CYP1A1/2 inhibitor α-naphthoflavone, CYP2A6 inhibitor methoxsalen, CYP2C19 inhibitor ticlopi-

DOI: 10.1021/acs.chemrestox.9b00112
Chem. Res. Toxicol. XXXX, XXX, XXX−XXX

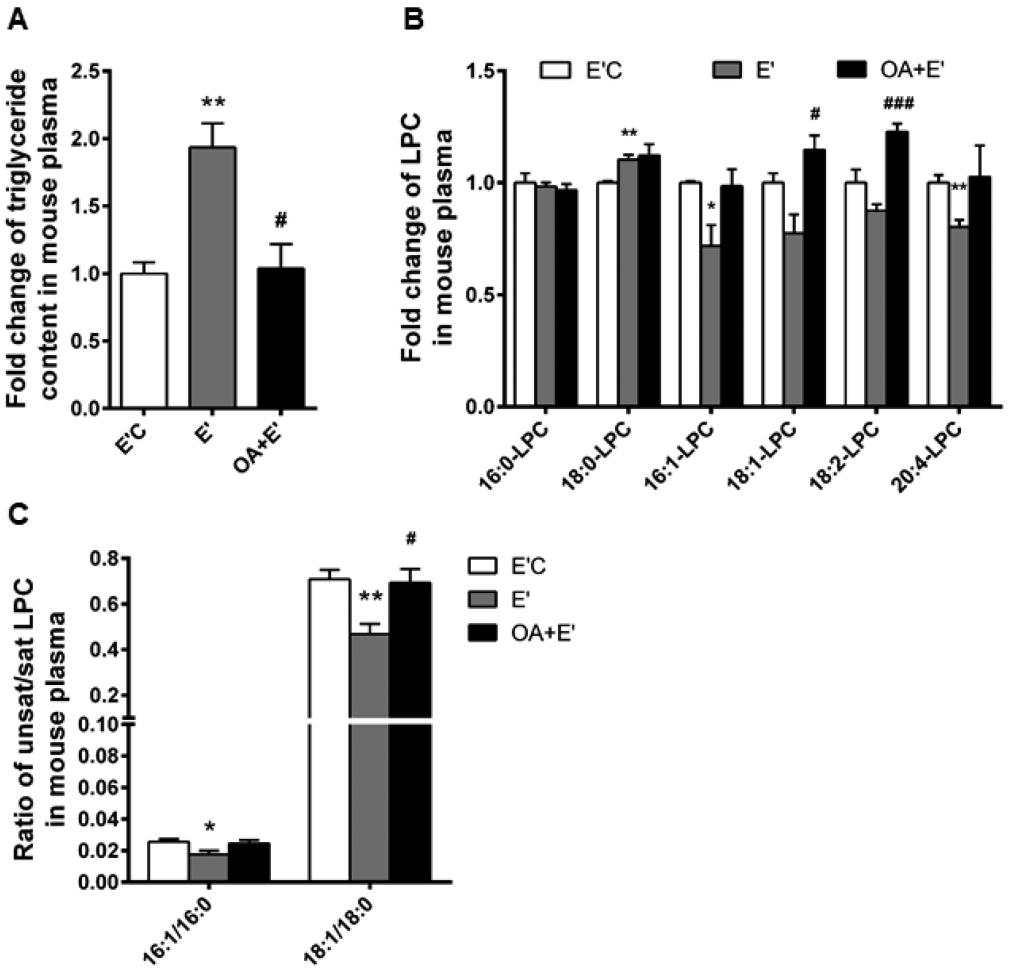

Figure 4. Oleic acid supplementary diet alleviated the metabolic disorder caused by 1′-hydroxyelemicin (E′). (A) Oleic acid reduced the TG content in mouse plasma. (B) Oleic acid supplementary diet recovered monounsaturated contents in mouse plasma. (C) The reduced ratio of monounsaturated-LPCs to saturated-LPCs balanced by oleic acid. *, $p < 0.05$ as compared to E′C group, **, $p < 0.01$ as compared to E′C group, $^{\#}$, $p < 0.05$ as compared to E′ group and $^{\#\#\#}$, $p < 0.001$ as compared to E′ group.

dine and CYP3A4/5 inhibitor ketoconazole showed relative higher inhibitory effects against 1′-hydroxyelemicin generation (Figure 6C).

Furthermore, the kinetic parameters of CYP1A1, CYP1A2, CYP2A6, CYP2C19, and CYP3A4 were measured. CYP1A1 exhibited high catalytic activity toward 1′-hydroxyelemicin generation (Figure S7A,B). The V_{max}, K_m, and V_{max}/K_m (catalytic efficiency) derived from the kinetic study revealed that CYP1A1 exhibited the maximum V_{max} value (1.80 ± 0.045 nmol • min^{-1} • nmol • CYP^{-1}) and the minimum K_m value (12.9 ± 1.26 μM), resulting in the highest catalytic efficiency (140 μL min^{-1} nmol CYP^{-1}; Table 1). In vitro experiment demonstrated CYP1A1 showed the highest catalytic activity toward 1′-hydroxyelemicin biotransformation, followed by CYP1A2 and CYP2C19. However, in untreated mice, CYP1A1 is expressed at very low levels in liver, while CYP1A2 is constitutively highly expressed in liver (4%). Taken together, CYP1A1 and CYP1A2 were considered as the major active enzymes for the formation of 1′-hydroxyelemicin in vitro and in vivo.

In order to verify the role of metabolic activation involved in elemicin induced hepatotoxicity, comparison of 1′-hydroxyelemicin- and elemicin-induced hepatotoxicity were performed at the same dose (100 mg/kg). 1′-Hydroxyelemicin treatment led to hepatomegaly, while, elemicin treatment did not result in hepatomegaly. These findings indicated reactive 1′-hydroxyelemicin showed higher hepatotoxicity than elemicin. In addition, the role of CYP1A inhibition in hepatotoxicity was performed in vivo. The CYP1A2 inhibitor alpha-naphthoflavone could significantly alleviate elemicin-induced hepatomegaly (Figure 8A). The ratios of 18:1-LPC/18:0-LPC and 16:1-LPC/16:0-LPC were increased in α-naphthoflavone and elemicin administered mice (Figure 8B), compared with elemicin treatment.

Molecular Docking of Elemicin into the Active Cavity of CYPs. In order to further validate the role of CYP enzymes in the metabolic activation of elemicin, the model of molecular docking was performed. The results indicated that the structure of elemicin can enter the active cavity of CYP1A1, CYP1A2, CYP2A6, CYP2C19, and CYP3A4 (Figures 7 and S8). In the docking of CYP1A1, elemicin could conjugate with CYP1A1 through two bonds; arene-hydrogen with the residue of Ala317 and side donor with the residue of Ser122 was discovered. Methyl and ethene moiety of elemicin can be well exposed in the active cavity of CYP1A1 (Figure 7A). In addition, elemicin could bind with Cys458 in the CYP1A2 active site via one arene-hydrogen bond (Figure 7B). Similarly, elemicin can bind with the Leu370 and Cys435 in CYP2A6 and CYP2C19 active site pockets, respectively, with the methyls of elemicin exposed (Figure 7C,D and Table 2). Only

DOI: 10.1021/acs.chemrestox.9b00112
Chem. Res. Toxicol. XXXX, XXX, XXX−XXX

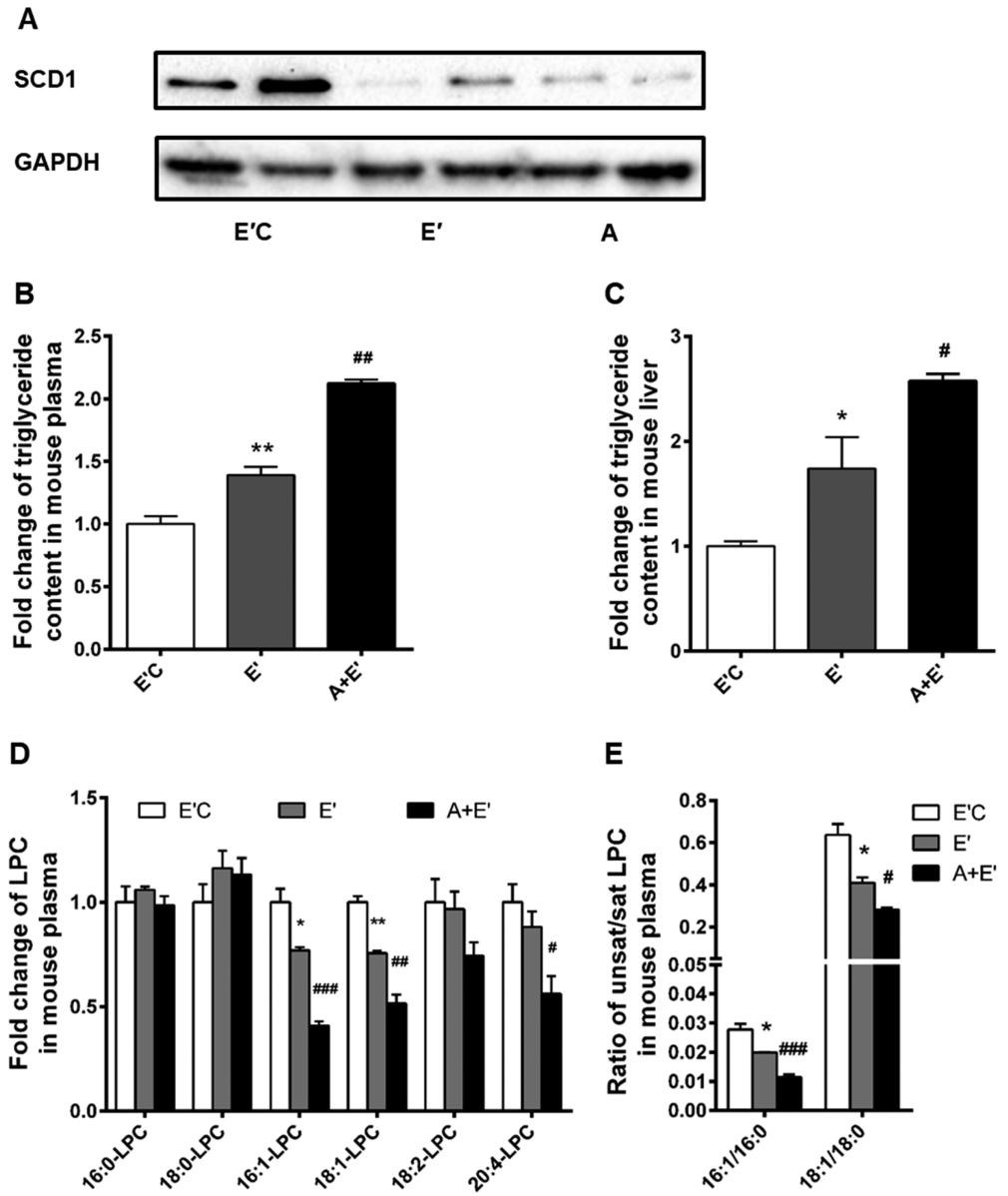

Figure 5. SCD1 inhibitor A939572 exacerbated the toxicity of 1′-hydroxyelemicin (E′). (A) Western blot analysis of SCD1. (B) A939572 significantly elevated TG content in mouse plasma after 1′-hydroxyelemicin treatment. (C) A939572 significantly elevated TG content in mouse liver after 1′-hydroxyelemicin treatment. (D) A939572 reduced monounsaturated-LPCs contents in mouse plasma. (E) Ratios of monounsaturated-LPCs to saturated-LPCs were reduced by A939572. *, $p < 0.05$ as compared to E′C group, **, $p < 0.01$ as compared to E′C group, #, $p < 0.05$ as compared to E′, group, ##, $p < 0.01$ as compared to E′ group and ###, $p < 0.001$ as compared to E′ group.

the ligand exposure in elemicin was observed in the binding mode of CYP3A4 (Figure 7E). The number of hydrogen bond between donor and acceptors demonstrated that CYP 1A1 exhibited stronger interaction with elemicin than the other CYPs (Table S3). Overall, CYP1A1 show the strongest affinity toward elemicin in silico.

DISCUSSION

In the present study, the potential hepatotoxicity of a three-week elemicin administration was evaluated in mice. Elemicin exposure at the dose of 500 mg/kg induced liver enlargement and increased serum and hepatic TG. GSH and GSSG were significantly decreased by elemicin, suggesting the metabolic production of an electrophilic metabolite. Similarly, its reactive 1′-hydroxyelemicin also caused the increased liver size and depletion of GSH and GSSG. When GSH was trapped with reactive metabolites, the total levels of GSH [GSH + GSSG] were decreased in a previous study.[25] The enlargement of hepatocytes was primarily observed around the central vein following elemicin and 1′-hydroxyelemicin treatment. Hepatomegaly is usually accompanied by a disorder of lipid metabolism.[26] Further study found that both elemicin and 1′-hydroxyelemicin treatment could inhibit the expression of SCD1 in liver, suggesting lipid dysregulation induced by elemicin and 1′-hydroxyelemicin (Figure 8).

UPLC-MS metabolomics analysis revealed that the metabolic balance of saturated LPCs and monounsaturated LPCs was disturbed in serum by both elemicin and 1′-hydroxyelemicin treatment. LPCs are phosphatide, which are the major lipid species in serum and have many important physiological functions.[27] The principal lipotoxic saturated fatty acids (SFA) in the liver are palmitic acid (C16:0) and

DOI: 10.1021/acs.chemrestox.9b00112
Chem. Res. Toxicol. XXXX, XXX, XXX−XXX

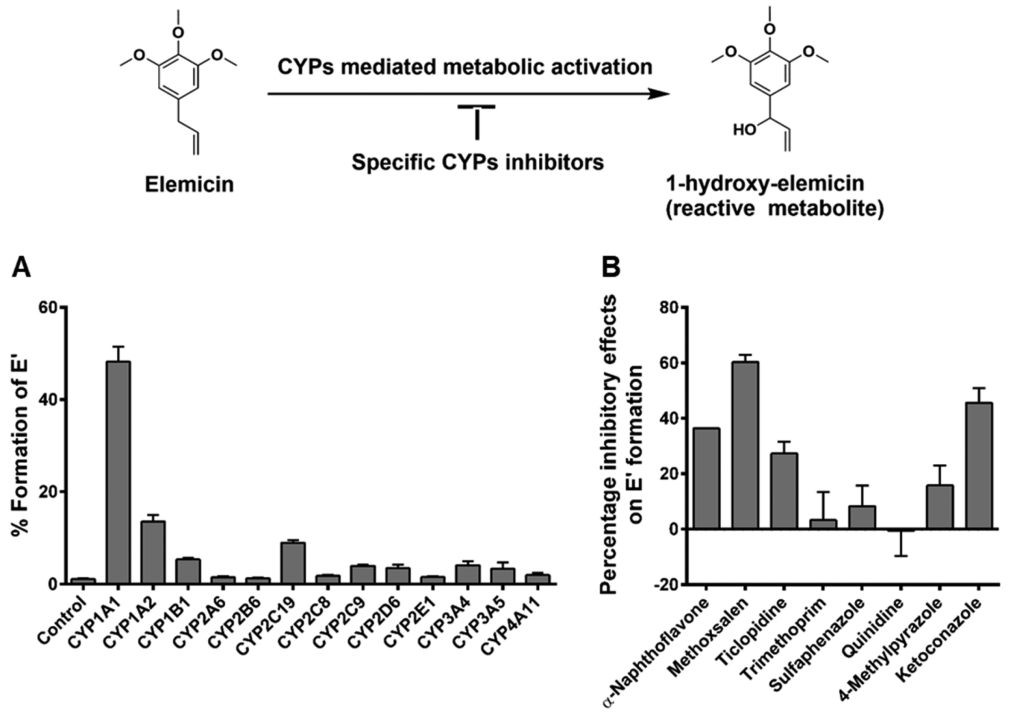

Figure 6. Determination of CYPS contributed to metabolic activation of elemicin. (A) Roles of CYPs in the formation of 1′-hydroxyelemicin. (B) Inhibitory effects of specific P450 inhibitors on the formation of 1′-hydroxyelemicin in MLMs incubations.

Table 1. Kinetic Constants of Recombined Human P450s for Elemicin Metabolism

enzyme	V_{max} (nmol min^{-1} nmol P450^{-1})[a]	K_m (μM)[a]	in vitro catalytic efficiency (μL min^{-1} nmol P450^{-1})[b]
CYP1A1	1.804 ± 0.045	12.880 ± 1.265	140.062
CYP1A2	0.402 ± 0.021	15.850 ± 3.067	25.363
CYP2A6	0.524 ± 0.110	1007.000 ± 293.000	0.520
CYP2C19	0.475 ± 0.012	43.430 ± 3.613	10.933
CYP3A4	0.262 ± 0.026	196.700 ± 46.190	1.332

[a]Mean values of three independent measurements ± SD. [b]In vitro catalytic efficiency = $V_{max}/K_m \times 1000$ μL.

stearic acid (C18:0), which can be transformed into the less lipotoxic monounsaturated fatty acids (MUFA) palmitoleate acid (C16:1) and oleate acid (C18:1). It was reported that the proportion of stearic acid and oleic acid could affect the growth and differentiation of cells through regulating the fluidity of biomembranes and the signal transduction process.[28]

The double bond in SFA is catalyzed by hepatic lipogenic rate-limiting enzymes SCD1, which is a key regulator of SFA and MUFA.[29,30] Since the liver is a principal organ for LPCs biosynthesis, the disorder of LPCs metabolism was ascribed to the inhibition of *Scd1* expression in liver. It is known that hepatic SCD1 abnormality is associated with hepatic steatosis, and SCD1 negatively correlated with inflammation via controlling the homeostasis of MUFA and SFA. In particular, inhibition of SCD1 aggravated responses to exogenous pro-inflammatory challenges in acute colitis.[31] Moreover, accumulation of SFA in *Scd1*-null mice enhanced inflammation via TLR4 signaling and promote atherosclerosis,[32] and loss of SCD1 attenuated adipose tissue inflammation,[33] suggesting that its expression was closely related to the formation and development of inflammation. As expected, the hepatic expression of the *Scd1* mRNA and SCD1 protein were inhibited by elemicin and 1′-hydroxyelemicin. Downregulation of *Scd1*was also observed in the binge ethanol-induced steatosis and hepatotoxicity.[34] A previous study demonstrated that SCD1 deficiency may lead to hepatic overaccumulation of lipids in nonalcoholic fatty liver disease,[24] indicating that TG accumulation might be induced by SCD1 inhibition. A previous study reported that the ratios of saturated-LPCs to monounsaturated-LPCs in mouse serum were decreased in the dextran sulfate sodium (DSS)-induced acute experimental colitis model, accompanied by *Scd1* suppression.[31] Here, further studies revealed that an oleic acid supplementary diet could recover the homeostasis of the LPCs metabolism and decrease plasma TG content. In contrast, the SCD1 inhibitor (A939572) exacerbated the increase of TG in plasma and liver by 1′-hydroxyelemicin and reduced proportion of unsaturated-LPCs. Therefore, the suppression of SCD1 may be responsible for liver toxicity of elemicin and 1′-hydroxyelemicin.

Many xenobiotics are converted to potential toxicants by transformation into reactive metabolites, resulting in hepatotoxicity and genotoxicity.[35] In particular, the hydroxylation of alkenylbenzenes at the 1′-position of the allyl side chain plays a crucial role in the formation of their genotoxicity,[11] which can be catalyzed and regulated by multiple CYPs. A previous study revealed that, in comparison with myristicin, 1′-hydroxymyristicin exhibited more significant genotoxicity and cytotoxicity.[16] 1′-Hydroxyelemicin can cause more hepatomegaly than elemicin at a dose of 100 mg/kg in this study, which was in agreement with the finding that metabolic activation enhances

DOI: 10.1021/acs.chemrestox.9b00112
Chem. Res. Toxicol. XXXX, XXX, XXX−XXX

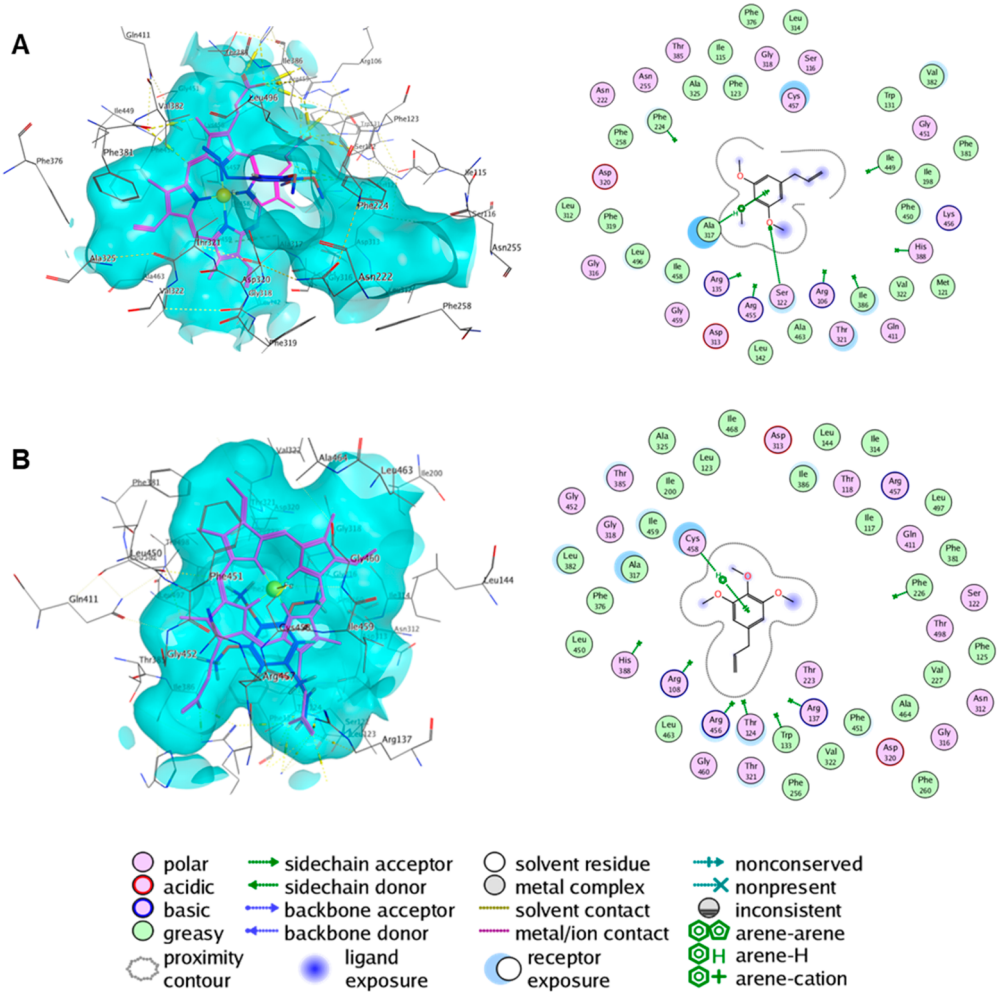

Figure 7. Molecular docking of elemicin with CYPs active cavity. (A) The docking conformation of elemicin into the active pockets of CYP1A1 and the diagrammatic sketch of interaction between elemicin and the amino acid residues of CYP1A1 pocket. (B) The docking conformation of elemicin into the active pockets of CYP1A2 and the diagrammatic sketch of interaction between elemicin and the amino acid residues of CYP1A2 pocket. Blue structure represents elemicin, and red structure represents endogenous ligand ferroheme of CYPs.

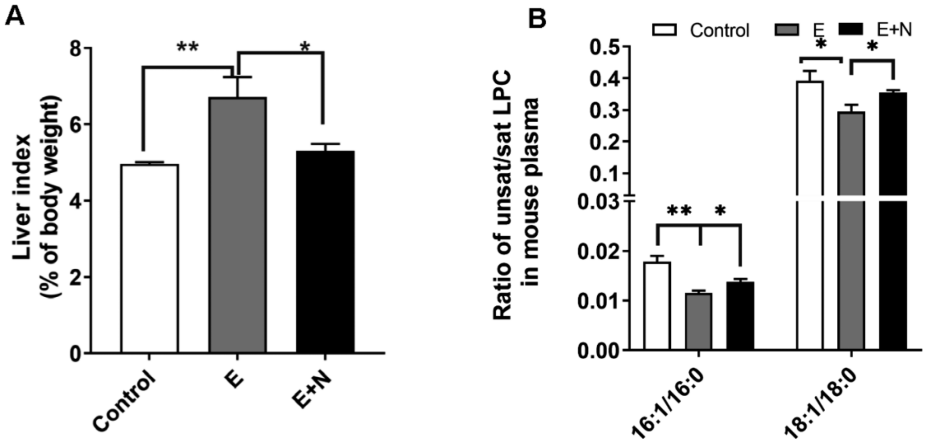

Figure 8. CYP1A2 inhibitor α-naphthoflavone can attenuate the susceptibility of mice to hepatomegaly of elemicin. (A) α-Naphthoflavone reduced elemicin induced hepatomegaly. (B) Ratio of monounsaturated-LPCs to saturated-LPCs.

its toxicity in cells.[16] The biotransformation of relatively inert chemicals into highly reactive intermediary metabolites, which can bind with GSH, nucleic acid and protein,[36] which is an initial event in many chemically induced toxicities. In this study, 1′-hydroxyelemicin also exhibited high reactivity leading to nonenzymatic capture with GSH, and formation of a GSH adduct.

It is well-known that phase I metabolic enzymes catalyze the bioactivation of xenobiotics. It was reported that CYP1A2 was the main enzyme responsible for the bioactivation of

DOI: 10.1021/acs.chemrestox.9b00112
Chem. Res. Toxicol. XXXX, XXX, XXX−XXX

methyleugenol.[37,38] CYP1A2 and CYP2A6 were identified as the major enzymes involving in the bioactivation of estragole.[11] Herein, recombinant human CYPs revealed that CYP1A1 and CYP1A2 contributed to the formation of 1′-hydroxyelemicin in vitro. Among the tested CYPs, CYP1A1 possessed the minimum K_m value, while CYP2A6 had the highest K_m value of 100 μM. By comparing with V_{max}/K_m rate of different CYPs, CYP1A1 showed most potent catalytic capability toward formation of 1′-hydroxyelemicin in vitro, followed by CYP1A2. Molecular docking of CYPs also revealed that CYP1A1 showed the strongest affinity with elemicin. Generally, CYP1A1 is not significantly expressed in liver of untreated mice and humans. Therefore, CYP1A2 is likely the major CYP contributing to the metabolic activation of elemicin in untreated mouse liver, which were also confirmed by CYP1A inhibition in vivo. The CYP1A2 inhibitor α-naphthoflavone could attenuate elemicin-induced hepatomegaly and metabolic disorder of lipids by inhibition of metabolic activation of elemicin, particularly in livers of mice exposed to ligands for the aryl-hydrocarbon receptor that induces expression of both CYP1A1 and CYP1A2.

In summary, the naturally occurring compound elemicin could induce the increased liver size. It was demonstrated that the inhibition of SCD1 was responsible in part for elemicin toxicity, and CYP1A1 and CYP1A2 likely contributed to the generation of 1′-hydroxyelemicin from elemicin. The potential liver toxicity of elemicin should be monitored if excessive consumption of foods and herbs rich in elemicin.

■ ASSOCIATED CONTENT

Supporting Information

The Supporting Information is available free of charge on the ACS Publications website at DOI: 10.1021/acs.chemrestox.9b00112.

(Figure S1) Plasma aminotransferase (ALT) activity after elemicin (E, 500 mg/kg) and 1′-hydroxyelemicin (E′, 100 mg/kg); (Figure S2) comparison between elemicin (E) and 1′-hydroxyelemicin (E′) toxicity at the oral dose of 100 mg/kg for 3 days; (Figure S3) reactive metabolite-GSH adduct in vivo and in vitro; (Figure S4) MS/MS spectra and fragmentation patterns of typical LPCs; (Figure S5) mRNA expression from genes related to LPC synthesis and metabolism; (Figure S6) influence of oleic acid supplementation on liver size and hepatic TG content; (Figure S7) plots of 1′-hydroxyelemicin formation from different elemicin concentrations; (Figure S8) molecular docking of elemicin with CYPs active cavity (PDF)

■ AUTHOR INFORMATION

Corresponding Author

*Tel: +86-871-65216953. E-mail: lifeib@mail.kib.ac.cn.

Author Contributions

▽These authors contributed equally to this work.

Funding

This work was supported by the National Key Research and Development Program of China (2017YFC1700906 and 2017YFC0906903), CAS "Light of West China" Program (Y72E8211W1), Kunming Institute of Botany (Y76E1211K1 and Y4662211K1), State Key Laboratory of Phytochemistry and Plant Resources in West China (52Y67A9211Z1), open funding of state key laboratory of Pharmaceutical Biotechnology, Nanjing University (KF-GN-201705), and postdoctoral funding from Yunnan Province.

Notes

The authors declare no competing financial interest.

■ REFERENCES

(1) Thai, T. H., Bazzali, O., Hoi, T. M., Tuane, N. A., Tomi, F., Casanova, J., and Bighelli, A. (2013) Chemical composition of the essential oils from two Vietnamese Asarum species: A. glabrum and A. cordifolium. *Nat. Prod. Commun. 8*, 235−238.

(2) De Vincenzi, M., De Vincenzi, A., and Silano, M. (2004) Constituents of aromatic plants: elemicin. *Fitoterapia 75*, 615−618.

(3) Martins, C., Rueff, J., and Rodrigues, A. S. (2018) Genotoxic alkenylbenzene flavourings, a contribution to risk assessment. *Food Chem. Toxicol. 118*, 861−879.

(4) Rossi, P. G., Bao, L., Luciani, A., Panighi, J., Desjobert, J. M., Costa, J., Casanova, J., Bolla, J. M., and Berti, L. (2007) E)-Methylisoeugenol and elemicin: antibacterial components of Daucus carota L. essential oil against Campylobacter jejuni. *J. Agric. Food Chem. 55*, 7332−7336.

(5) Surveswaran, S., Cai, Y., Corke, H., and Sun, M. (2007) Systematic evaluation of natural phenolic antioxidants from 133 Indian medicinal plants. *Food Chem. 102*, 938−953.

(6) Sajjadi, S., Shokoohinia, Y., and Hemmati, S. (2012) Antivirial activity of elemicin from Peucedanum pastinacifolium. *Cytokine 43*, 278−278.

(7) Martins, C., Doran, C., Laires, A., Rueff, J., and Rodrigues, A. S. (2011) Genotoxic and apoptotic activities of the food flavourings myristicin and eugenol in AA8 and XRCC1 deficient EM9 cells. *Food Chem. Toxicol. 49*, 385−392.

(8) Kaledin, V. I., Pakharukova, M., Pivovarova, E. N., Kropachev, K., Baginskaia, N. V., Vasil'eva, E. D., Il'nitskaia, S. I., Nikitenko, E. V., Kobzev, V. F., and Merkulova, T. I. (2010) Effect of hepatocarcinogenicity of estragole on the glucocorticoid-mediated induction of liver-specific enzymes and the activity of the transcription factors FOXA and HNF4 in the liver of mouse and rat. *Biofizika 55*, 326−335.

(9) Wiseman, R. W., Miller, E. C., Miller, J. A., and Liem, A. (1987) Structure-activity studies of the hepatocarcinogenicities of alkenylbenzene derivatives related to estragole and safrole on administration to preweanling male C57BL/6J x C3H/HeJ F1 mice. *Cancer Res. 47*, 2275−2283.

(10) Williams, G. M., Iatropoulos, M. J., Jeffrey, A. M., and Duan, J. D. (2013) Methyleugenol hepatocellular cancer initiating effects in rat liver. *Food Chem. Toxicol. 53*, 187−196.

(11) Jeurissen, S. M., Punt, A., Boersma, M. G., Bogaards, J. J., Fiamegos, Y. C., Schilter, B., van Bladeren, P. J., Cnubben, N. H., and Rietjens, I. M. (2007) Human cytochrome p450 enzyme specificity for the bioactivation of estragole and related alkenylbenzenes. *Chem. Res. Toxicol. 20*, 798−806.

(12) Borchert, P., Miller, J. A., Miller, E. C., and Shires, T. K. (1973) 1'-Hydroxysafrole, a proximate carcinogenic metabolite of safrole in the rat and mouse. *Cancer Res. 33*, 590−600.

(13) Hasheminejad, G., and Caldwell, J. (1994) Genotoxicity of the alkenylbenzenes alpha- and beta-asarone, myristicin and elimicin as determined by the UDS assay in cultured rat hepatocytes. *Food Chem. Toxicol. 32*, 223−231.

(14) Miller, E. C., Swanson, A. B., Phillips, D. H., Fletcher, T. L., Liem, A., and Miller, J. A. (1983) Structure-activity studies of the carcinogenicities in the mouse and rat of some naturally occurring and synthetic alkenylbenzene derivatives related to safrole and estragole. *Cancer Res. 43*, 1124−1134.

(15) Kobets, T., Duan, J. D., Brunnemann, K. D., Etter, S., Smith, B., and Williams, G. M. (2016) Structure-Activity Relationships for DNA Damage by Alkenylbenzenes in Turkey Egg Fetal Liver. *Toxicol. Sci. 150*, 301−311.

(16) Marabini, L., Neglia, L., Monguzzi, E., Galli, C. L., and Marinovich, M. (2017) Assessment of toxicity of myristicin and 1'-

DOI: 10.1021/acs.chemrestox.9b00112
Chem. Res. Toxicol. XXXX, XXX, XXX−XXX

hydroxymyristicin in HepG2 cell line. *J. Pharmacol. Toxicol. 12*, 170−179.
(17) van den Berg, S. J., Punt, A., Soffers, A. E., Vervoort, J., Ngeleja, S., Spenkelink, B., and Rietjens, I. M. (2012) Physiologically based kinetic models for the alkenylbenzene elemicin in rat and human and possible implications for risk assessment. *Chem. Res. Toxicol. 25*, 2352−2367.
(18) Solheim, E., and Scheline, R. R. (1980) Metabolism of alkenebenzene derivatives in the rat. III. Elemicin and isoelemicin. *Xenobiotica 10*, 371−380.
(19) Yang, X. N., Liu, X. M., Fang, J. H., Zhu, X., Yang, X. W., Xiao, X. R., Huang, J. F., Gonzalez, F. J., and Li, F. (2018) PPARα mediates the hepatoprotective effects of nutmeg. *J. Proteome Res. 17*, 1887−1897.
(20) Yang, X.-N., Lv, Q.-Q., Zhao, Q., Li, X.-M., Yan, D.-M., Yang, X.-W., and Li, F. (2017) Metabolic profiling of myrislignan by UPLC-ESI-QTOFMS-based metabolomics. *RSC Adv. 7*, 40131−40140.
(21) Sun, Y., Yao, T., Li, H., Peng, Y., and Zheng, J. (2017) In vitro and in vivo metabolic activation of berbamine to quinone methide intermediate. *J. Biochem. Mol. Toxicol. 31*, e21876.
(22) Amaya, G. M., Durandis, R., Bourgeois, D. S., Perkins, J. A., Abouda, A. A., Wines, K. J., Mohamud, M., Starks, S. A., Daniels, R. N., and Jackson, K. D. (2018) Cytochromes P450 1A2 and 3A4 Catalyze the Metabolic Activation of Sunitinib. *Chem. Res. Toxicol. 31*, 570−584.
(23) Wang, Y. K., Xiao, X. R., and Xu, K. P. (2018) Metabolic profiling of the anti-tumor drug regorafenib in mice. *J. Pharm. Biomed. Anal. 159*, 524−535.
(24) Li, Z. Z., Berk, M., McIntyre, T. M., and Feldstein, A. E. (2009) Hepatic lipid partitioning and liver damage in nonalcoholic fatty liver disease: role of stearoyl-CoA desaturase. *J. Biol. Chem. 284*, 5637−5644.
(25) Sasaki, E., Matsuo, K., Iida, A., Tsuneyama, K., Fukami, T., Nakajima, M., and Yokoi, T. (2013) A novel mouse model for phenytoin-induced liver injury: involvement of immune-related factors and P450-mediated metabolism. *Toxicol. Sci. 136*, 250−263.
(26) Bharath, N., Ivan, L., Timea, C., Jan, P., Christian, M., Karen, K., Donna, C., Pranoti, M., and Gyongyi, S. (2011) Hepatocyte-specific hypoxia-inducible factor-1α is a determinant of lipid accumulation and liver injury in alcohol-induced steatosis in mice. *Hepatology 53*, 1526−1537.
(27) Croset, M., Brossard, N., Polette, A., and Lagarde, M. (2000) Characterization of plasma unsaturated lysophosphatidylcholines in human and rat. *Biochem. J. 345*, 61−67.
(28) Ntambi, J. M. (1999) Regulation of stearoyl-CoA desaturase by polyunsaturated fatty acids and cholesterol. *J. Lipid Res. 40*, 1549−1558.
(29) Singh, V., Chassaing, B., Zhang, L., San Yeoh, B., Xiao, X., Kumar, M., Baker, M. T., Cai, J., Walker, R., Borkowski, K., Harvatine, K. J., Singh, N., Shearer, G. C., Ntambi, J. M., Joe, B., Patterson, A. D., Gewirtz, A. T., and Vijay-Kumar, M. (2015) Microbiota-Dependent Hepatic Lipogenesis Mediated by Stearoyl CoA Desaturase 1 (SCD1) Promotes Metabolic Syndrome in TLR5-Deficient Mice. *Cell Metab. 22*, 983−996.
(30) Dobrzyn, P., Dobrzyn, A., Miyazaki, M., Cohen, P., Asilmaz, E., Hardie, D. G., Friedman, J. M., and Ntambi, J. M. (2004) Stearoyl-CoA desaturase 1 deficiency increases fatty acid oxidation by activating AMP-activated protein kinase in liver. *Proc. Natl. Acad. Sci. U. S. A. 101*, 6409−6414.
(31) Chen, C., Shah, Y. M., Morimura, K., Krausz, K. W., Miyazaki, M., Richardson, T. A., Morgan, E. T., Ntambi, J. M., Idle, J. R., and Gonzalez, F. J. (2008) Metabolomics reveals that hepatic stearoyl-CoA desaturase 1 downregulation exacerbates inflammation and acute colitis. *Cell Metab. 7*, 135−147.
(32) B Fessler, M., Rudel, L., and Mark Brown, J. (2009) Fessler MB, Rudel LL, Brown JM. Toll-like receptor signaling links dietary fatty acids to the metabolic syndrome. *Curr. Opin. Lipidol. 20*, 379−385.
(33) Liu, X., Miyazaki, M., Flowers, M. T., Sampath, H., Zhao, M., Chu, K., Paton, C. M., Joo, D. S., and Ntambi, J. M. (2010) Loss of Stearoyl-CoA desaturase-1 attenuates adipocyte inflammation: effects of adipocyte-derived oleate. *Arterioscler., Thromb., Vasc. Biol. 30*, 31−38.
(34) Choi, S., Gyamfi, A. A., Neequaye, P., Addo, S., Gonzalez, F. J., and Gyamfi, M. A. (2018) Role of the pregnane X receptor in binge ethanol-induced steatosis and hepatotoxicity. *J. Pharmacol. Exp. Ther. 365*, 165.
(35) Shu-Feng, Z., Charlie Changli, X., Xue-Qing, Y., and Guangji, W. (2007) Metabolic activation of herbal and dietary constituents and its clinical and toxicological implications: an update. *Curr. Drug Metab. 8*, 526−553.
(36) Srivastava, A., Maggs, J. L., Antoine, D. J., Williams, D. P., Smith, D. A., and Park, B. K. (2010) Role of Reactive Metabolites in Drug-Induced Hepatotoxicity. *Handb. Exp. Pharmacol. 196*, 165−194.
(37) Gardner, I., Wakazono, H., Bergin, P., De, W. I., Beaune, P., Kenna, J. G., and Caldwell, J. (1997) Cytochrome P450 mediated bioactivation of methyleugenol to 1'-hydroxymethyleugenol in Fischer 344 rat and human liver microsomes. *Carcinogenesis 18*, 1775−1783.
(38) Jeurissen, S. M. F., Bogaards, J. J. P., Boersma, M. G., Horst, J. P. F. T., and Awad, H. M. (2006) Human cytochrome p450 enzymes of importance for the bioactivation of methyleugenol to the proximate carcinogen 1'-hydroxymethyleugenol. *Chem. Res. Toxicol. 19*, 111−116.

DOI: 10.1021/acs.chemrestox.9b00112
Chem. Res. Toxicol. XXXX, XXX, XXX−XXX